Mon. Not. R. Astron. Soc. **000**, 1–?? (2012) Printed 1 October 2014 (MN LATEX style file v2.2)

The high optical polarization in the Be/X-ray binary EXO 2030+375

P. Reig[1,2⋆], D. Blinov[2,3], I. Papadakis[2,1], N. Kylafis[2,1], K. Tassis[2,1]
[1] *IESL, Foundation for Research and Technology-Hellas, GR-71110 Heraklion, Crete, Greece*
[2] *Department of Physics & Institute of Theoretical & Computational Physics, University of Crete, PO Box 2208, GR-710 03, Heraklion, Crete, Greece*
[3] *Astronomical Institute, St. Petersburg State University,Universitetsky pr. 28, Petrodvoretz, 198504 St. Petersburg, Russia*

arXiv:1409.8411v1 [astro-ph.SR] 30 Sep 2014

Accepted ??. Received ??; in original form ??

ABSTRACT

Polarization in classical Be stars results from Thomson scattering of the unpolarized light from the Be star in the circumstellar disc. Theory and observations agree that the maximum degree of polarization from isolated Be stars is $\lesssim$4%. We report on the first optical polarimetric observations of the Be/X-ray binary EXO 2030+375. We find that the optical (*R* band) light is strongly linearly polarized with a degee of polarization of 19%, the highest ever measured either in a classical or Be/X-ray binary. We argue that the interstellar medium cannot account for this high polarization degree and that a substantial amount must be intrinsic to the source. We propose that it may result from the alignment of non-spherical ferromagnetic grains in the Be star disc due to the strong neutron star magnetic field.

Key words: X-rays: binaries – stars: neutron – stars: binaries close – stars: emission line, Be

1 INTRODUCTION

Be/X-ray binaries (BeXB) are a subclass of high-mass X-ray binaries that consist of a Be star and a neutron star (see e.g. Reig 2011). The mass donor is a relatively massive ($\gtrsim$ 10 $M_\odot$) and fast-rotating (∼80% of break-up velocity) Be star, whose equator is surrounded by a disc formed from photospheric plasma ejected by the star. The equatorial disc is believed to be Keplerian and supported by viscosity (Rivinius, Carciofi & Martayan 2013). The accreting component is a strongly magnetized neutron star. Matter from the disc is transferred to the neutron star, latched onto the magnetic field lines and deposited onto a very small fraction (∼1%) of the neutron star surface, the polar caps, where its kinetic energy is converted into X-rays.

Be stars are also observed as single objects, that is, not forming part of a binary system (Porter & Rivinius 2003; Rivinius, Carciofi & Martayan 2013). In principle, the underlying Be star in a BeXB and in the isolated Be share the same physical properties (mass, radius, luminosity, temperature) for the same spectral type. However, there is strong evidence that the discs around Be stars in BeXB are strongly affected by the neutron star, resulting in more compact and denser discs (Okazaki et al. 2002; Reig 2011).

The three observational properties that chartacterise Be stars are emission lines (which give the name of the class, i.e. "e" stands for emission), infrared excess and polarized light. Partially or totally filled-in emission lines are typically the dominant feature in the optical and infrared spectra of such stars. The shape and strength of the Hα line are useful indicators of the state of the disc. Photometrically, Be stars present redder colors than normal, i.e. non-emitting, B stars of the same spectral type. Also, Be stars are brighter in the infrared than B stars, an effect known as infrared excess. Optical polarized light at 1–3% is a common feature among isolated Be stars (Yudin 2001).

All these three phenomena are explained by radiation processes taking place in the extended circumstellar disc. Emission lines result from continuous hydrogen recombination of atoms excited by the radiation emitted from the massive star. Similarly, the infrared excess is due to free-bound and free-free radiation in the ionized circumstellar disc, with no evidence for dust (Gehrz, Hackwell & Jones 1974; Dachs, Kiehling & Engels 1988). The continuum polarization is attributed to Thomson scattering of unpolarized starlight in the disc. The maximum polarization level in an axisymmetric circumstellar disc predicted by single-scattering plus attenuation models is about 2% (Waters & Marlborough 1992). Although this value generally agrees well with the observations (Yudin 2001), the single-scattering calculation are too simplistic as they assume optically thin discs. For gaseous discs with extended optically thick regions, multiple scattering significantly modifies the resultant continuous polarization. Monte Carlo simulations allowing for multi-scattering show that the optical polarization level increases as the optical depth increases, reaches a maximum around to 3–4%, and then decreases for further increase of the optical depth (Wood et al. 1996; Halonen, Mackay & Jones 2013).

EXO 2030+375 is a BeXB that has now been observed for almost 30 years since its discovery by *EXOSAT* in 1985 (Parmar et al. 1989). During this time, it underwent two giant X-ray outbursts, in 1985 and 2006, and numerous orbitally-modulated ($P_{\rm orb}$ = 46.0207 ± 0.0004 days) outbursts (Wilson, Finger & Camero-Arranz 2008). The optical counterpart

⋆ E-mail: pau@physics.uoc.gr

Table 1. Robopol observations of EXO 2030+375. The polarization degree and angle were calculated as $PD = \sqrt{q^2 + u^2}$ and $PA = 0.5 \tan^{-1}(u/q)$.

Source	Date	JD	Orbital phase†	q	u	PD (%)	PA (°)	$N_{obs} \times t$ (s)
EXO 2030+375	2013-10-06	2456572.3914	0.92	0.029±0.015	0.193±0.015	19.6±1.5	40.8±2.2	4×150
EXO 2030+375	2013-10-21	2456587.3997	0.25	0.026±0.009	0.188±0.010	19.0±1.0	41.0±1.4	6×300
EXO 2030+375	2013-10-29	2456595.3656	0.42	0.032±0.010	0.182±0.010	18.5±1.0	40.0±1.5	7×200
EXO 2030+375	2014-05-15	2456793.5892	0.73	0.046±0.071	0.200±0.021	21.3±2.0	35.2±2.6	6×180
EXO 2030+375	2014-06-22	2456831.5212	0.55	0.019±0.012	0.184±0.011	18.5±1.2	42.0±1.9	6×125
EXO 2030+375	2014-08-01	2456871.5297	0.42	0.022±0.021	0.174±0.021	17.6±2.1	41.4±3.3	5×100

†: Orbital solution from Wilson, Finger & Camero-Arranz (2008)

Table 2. Robopol observations of four field stars in the vicinity of EXO 2030+375.

Source	Date	JD	q	u	PD (%)	PA (°)	Distance from target (")
Star 1	2014-06-19	2456828.5387	0.014±0.009	0.057±0.009	5.9±0.9	38±4	57
Star 2	2014-06-13	2456822.4453	0.008±0.005	0.013±0.007	1.5±0.7	30±14	90
Star 3	2014-05-20	2456798.5464	0.009±0.009	0.004±0.009	1.0±0.9	13±25	24
Star 4	2014-06-21	2456830.4945	0.058±0.018	0.038±0.007	7.0±1.5	17±5	40

Table 3. Photometric observations of EXO 2030+375 and nearby stars.

Object	B	V	R	I
2011-08-27 ; JD 2,455,801.38				
EXO 2030+375	22.08 ± 0.16	19.31 ± 0.03	17.25 ± 0.02	15.16 ± 0.02
Star 1	15.84 ± 0.02	14.97 ± 0.02	14.50 ± 0.02	14.04 ± 0.02
Star 2	15.63 ± 0.02	14.76 ± 0.02	14.28 ± 0.02	13.81 ± 0.02
Star 3	20.06 ± 0.03	18.27 ± 0.02	17.26 ± 0.02	16.34 ± 0.02
Star 4	21.45 ± 0.10	18.62 ± 0.02	16.74 ± 0.02	15.01 ± 0.02
2014-07-17 ; JD 2,456,856.31				
EXO 2030+375	21.86 ± 0.10	19.41 ± 0.02	17.31 ± 0.01	15.23 ± 0.02
Star 1	15.85 ± 0.01	15.01 ± 0.01	14.53 ± 0.02	14.06 ± 0.02
Star 2	15.64 ± 0.01	14.80 ± 0.01	14.31 ± 0.02	13.84 ± 0.02
Star 3	20.07 ± 0.03	18.33 ± 0.02	17.28 ± 0.02	16.41 ± 0.02
Star 4	21.30 ± 0.08	18.65 ± 0.02	16.76 ± 0.02	15.05 ± 0.02
2014-08-20 ; JD 2,456,890.52				
EXO 2030+375	22.12 ± 0.17	19.43 ± 0.03	17.29 ± 0.01	15.29 ± 0.03
Star 1	15.83 ± 0.02	15.02 ± 0.02	14.55 ± 0.02	14.09 ± 0.03
Star 2	15.70 ± 0.02	14.81 ± 0.02	14.33 ± 0.02	13.86 ± 0.03
Star 3	20.04 ± 0.03	18.32 ± 0.02	17.30 ± 0.02	16.37 ± 0.03
Star 4	21.32 ± 0.08	18.65 ± 0.02	16.76 ± 0.02	15.09 ± 0.03

is a highly reddened V=19.6 B0Ve star (Motch & Janot-Pacheco 1987; Coe et al. 1988).

In this work, we present the results of the first polarimetric observations of EXO 2030+375 in the optical band and report the discovery of an unexpected high polarization degree.

2 OBSERVATIONS

Photometry and polarimetry were obtained with the 1.3 m telescope of the Skinakas Observatory in Crete (Greece), which has a modified Ritchey-Chretien optical system with a 129 cm primary, 45 cm secondary, and $f = 7.54$.

2.1 Polarimetric observations

Polarimetric observations in the R band were made with the Robopol photopolarimeter (Ramaprakash et al. 2014, in preparation) attached to the focus of the telescope, on the nights indicated in Table 1. Robopol is a 4-channel imaging photopolarimeter. The incident light is split in two beams, each half incident on a half-wave retarder followed by a Wollaston prism. Every point in the sky is thereby projected to four points on the CCD. The CCD chip is an ANDOR DW436 2048×2048 with pixel size 13.5 μm, giving a field of view of $13' \times 13'$. The photon counts, measured using aperture photometry, in each spot are used to calculate the U and Q parameters of linear polarization. The fast axis of the half-wave retarder in front of the first prism is rotated by 67.5° with respect to the other retarder. To optimize the instrument sensitivity a mask is placed in the telescope focal plane. The mask has a cross-shaped aperture in the center where the target source is placed. The data were reduced following the pipeline procedure described in King et al. (2014). In the instrument reference frame, the horizontal channel measures the $u = U/I$ fractional Stokes parameter, while the vertical channel measures the $q = Q/I$ parameter, simultaneously, with a single exposure.

In addition to the BeXB EXO 2030+375, we also observed four nearby stars, which in the target images are hidden behind the mask. We chose these stars because of their proximity to the target, their isolation from nearby stars that could cause confusion, and because they cover all four directions around the target. The results of the polarimetric observations are shown in Table 2.

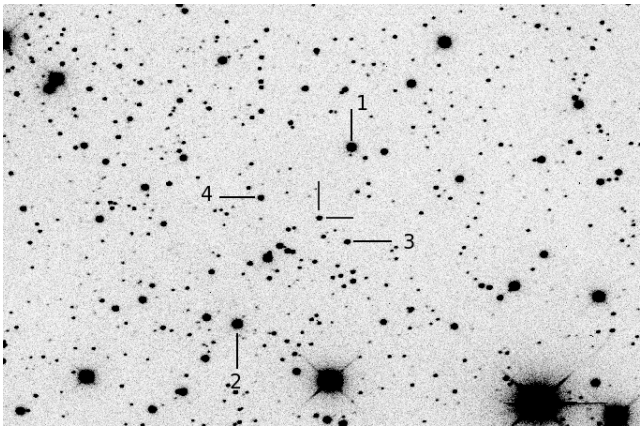

Figure 1. Optical (R band) field (7.5 × 4.2) arcmin around the BeXB EXO 2030+375. The four reference stars for which polarization was measured are indicated, together with the target.

2.2 Photometric observations

Johnson-Cousins-Bessel *BVRI* photometric observations were made of the field around EXO 2030+375. We obtained the magnitudes of the target and the four nearby stars for which polarimetry was obtained (Table 3). The telescope was equipped with a 2048×2048 ANDOR DZ436 CCD with a 13.5 μm pixel size (corresponding to 0.28 arcsec on the sky) providing a field of view of 9.5 arcmin × 9.5 arcmin. Reduction of the data was carried out in the standard way using the IRAF tools for aperture photometry. The photometry was accurately corrected for colour equations and transformed to the standard system using nightly observations of standard stars from Landolt's catalogue (Landolt 1992, 2009). Usually, the error of the photometry is calculated as the root-mean-square of the difference between the derived final calibrated magnitudes of the standard stars and the magnitudes of the catalogue. However, because of the faintness of the target and some of the nearby stars, we took the error to be the larger of the root-mean-square and the uncertainty obtained from the signal-to-noise ratio ($\sigma_B = 1.086/SNR$).

3 RESULTS AND DISCUSSION

We performed polarimetric observations of the BeXB EXO 2030+375 at six different epochs and found that the optical light in the R band is highly linearly polarized. No evidence for variability is observed neither in the degree of polarization nor in the polarization angle, with weighted average values of $P(\%) = 18.9 \pm 0.5$ and $\chi = 40.4^\circ \pm 0.8$, respectively . This is the highest polarization level ever measured in a Be star. Before attempting to find a mechanism to explain such a large polarization degree, we must assess whether the interstellar medium (ISM) can account for the measured polarization. Because the polarization of the interstellar medium is closely related to the amount of extinction, we first estimate the color excess of EXO 2030+375 from our photometry.

The observed colour of EXO 2030+375 is $(B-V) = 2.6 \pm 0.1$ (Table 3), while the expected one for a B0V star is $(B-V)_0 = -0.29$ (Fitzgerald 1970; Gutierrez-Moreno 1979; Wegner 1994). Thus we derive a colour excess of $E(B-V) = 2.9 \pm 0.1$ or visual extinction $A_V = R \times E(B-V) = 9.0 \pm 0.3$, where the standard extinction law $R = 3.1$ was assumed. In a Be star, the total measured reddening is made up of two components: one produced mainly by dust in the interstellar space along the line of sight and another produced by the circumstellar gas around the Be star. The contribution of the circumstellar reddening to the color excess $E(B-V)$ has been estimated in isolated Be stars to be $\lesssim$0.1 mag (Dachs, Kiehling & Engels 1988). To account for this extra reddening, we increased the error in $E(B-V)$ to 0.2 mag. Thus we finally derive $E(B-V) = 2.9 \pm 0.2$ mag.

An important point to estimate the amount of polarization from the ISM is the distance to the source. The distance to EXO 2030+375 is rather uncertain. The first optical observations could only constrain the distance to be in the range 2–7 kpc due to the unknown spectral type (Motch & Janot-Pacheco 1987). When optical spectroscopy was performed and a confirmation that the optical counterpart to EXO 2030+375 was indeed a Be star, then the maximum distance was proposed to be less than 4 kpc, assuming an overestimated value of $M_V = -5$ (Janot-Pacheco, Motch & Pakull 1988). The distance derived from fits of various accretion torque models to the X-ray luminosity versus spin rate relation agrees with the range 4–5 kpc (Parmar et al. 1989; Reynolds et al. 1996). However, Wilson et al. (2002) suggested a distance of ∼7 kpc using the relationship between extinction and distance for objects in the Galactic plane. Using our photometric data and taking the most recent absolute magnitude calibration for a B0Ve star, $M_V = -3.9 \pm 0.5$ (Wegner 2006), we find $d = 7 \pm 3$ kpc. The error of 0.5 magnitudes in M_V mainly accounts for the uncertainty in the spectral classification. The error in the distance was obtained by propagating the errors in $E(B-V)$, V, and M_V.

3.1 Interstellar polarization

Although we present the first polarimetric observations in the optical band, it is not the first time that polarization has been measured in EXO 2030+375. Norton et al. (1994) performed a multi-wavelength analysis of EXO 2030+375 during a normal outburst and reported on infrared polarimetric observations with the IRCAM infrared camera in the J and K bands. They measured average polarization fraction of 10.0 ± 0.6% in the J band and 4.2 ± 0.2% in the K band. Norton et al. (1994) suggested that the most likely origin of most of the measured polarization is the interstellar medium, although an intrinsic component of about 3% in J and 1% in K could not be ruled out. They based their conclusions on the average relationships between interstellar polarization and extinction (Serkowski, Mathewson & Ford 1975; Whittet & van Breda 1978) and the fact that interstellar polarization over 10% in the J band has been observed in OH/IR stars (Jones & Gehrz 1990).

In what follows, we present evidence that the ISM cannot account for the entire observed optical polarizaton in EXO 2030+375.

- *Polarization-extinction relationship*. The relationship between polarization and extinction has been studied by a number of authors (Hiltner 1956; Serkowski, Mathewson & Ford 1975; Jones 1989; Fosalba et al. 2002). These studies show that the polarization fraction increases as the extinction increases, albeit with a large scatter. In fact, rather than a neat correlation, there is an ensemble of points for the same or similar extinction. As the extinction increases, the maximum also increases.

Hiltner (1956) found this limit in $P_{\max}/A_V = 2.76\%$, similar to that by Serkowski, Mathewson & Ford (1975), who found $P_{\max}/E(B-V) = 9\%$. Note that the data used to build these relations are based on stars with $E(B-V) \lesssim 1$, hence relatively close to our Sun, and that the maximum envelope represents optimum align-

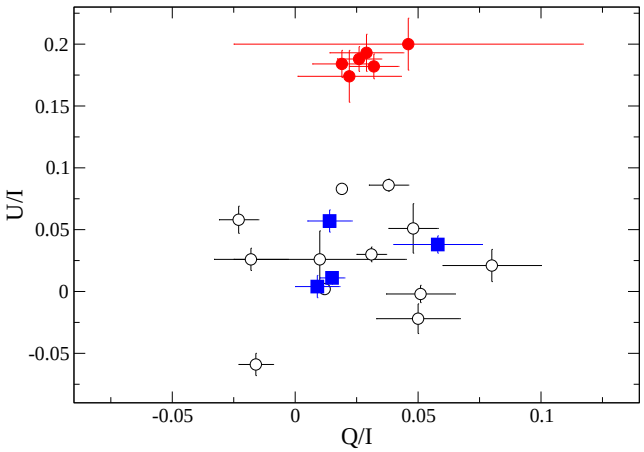

Figure 2. $q-u$ diagram. Black open circles are field stars. Blue filled squares correspond to the four stars for which dedicated pointed observation were made. The EXO 2030+375 measurements are indicated by red filled circles.

ment efficiency, that is, it arises on sight lines where the magnetic field is uniform, highly ordered, and where the dust grains are completely alligned. The allignment and uniformity of the magnetic field is expected to disappear as the line of sight crosses more and more interstellar dust clouds. Thus the more distant objects are expected to suffer from strong depolarization. This effect is apparent in the $P_{\rm max} - E(B-V)$ plots (Serkowski, Mathewson & Ford 1975) or, equivalently the $P_{\rm max} - A_V$ plots (Hiltner 1956), where one can see that the larger the extinction, the further away from the maximum line the star is. It looks like there is a turn over at about 6–7%. Using a much larger sample of stars, Fosalba et al. (2002) found that the observed mean correlation between extinction and ISM polarization is much smaller than what it is expected from interstellar dust grains completely aligned under a purely regular external magnetic field. Using their relation, $P_{\rm max,ISM}(\%) = 3.5\,E(B-V)^{0.8}$, the maximum contribution of the ISM to the measured polarization towards EXO 2030+375 would be $P_{\rm ISM} = 9\%$. Fosalba et al. (2002) also found that the polarization degree as a function of distance shows a maximum at $\sim 2-3\%$ for stars at 2–4 kpc and then decreases slightly for more distant objects up to 6 kpc.

These are average relationships obtained by measuring the polarization degree of a large number of stars in *all directions* of the Galaxy. However, the polarization degree strongly depends on the galactic longitude, with two maxima and two minima. The two minima are found at 50–70° and 230–250°, while the two maxima at 130–140° and 320–330° (Krautter 1980; Fosalba et al. 2002). The galactic coordinates of EXO 2030+375 are $l = 77.15°$ and $b = -1.24°$. At that longitude, $P(\%)/A_v \sim 1.0$ (Krautter 1980). Taking $E(B-V) = 2.9$ mag and assuming $R_V = 3.1$, the average polarization in the line of sight to EXO 2030+375 would be $P_{\rm ISM} \sim 9\%$.

- *Planck's polarization maps*. The Planck survey has shown that the polarization fraction in the galactic plane at 353 GHz is only a few percent (see Fig.4 in Planck Collaboration et al. 2014a). Moreover, the polarization fraction decreases with increasing column density. There is a sharp decline in polarization fraction starting at $N_H = 2\times10^{22}$ cm^{-2}, which corresponds to $A_V = 10$ mag, that is, approximately the extinction of EXO 2030+375. At this A_V, $p \sim 5\%$. The decrease of polarization fraction towards large column densities is interpreted as being due to depolarization, that is, a gradual loss of alignment of dust grains or to fluctuations in the orientation of the magnetic field along the line of sight. Note that this p refers to the polarization fraction at 353 GHz. However, the submillimitre polarization intensity, P_S, at 353 GHz is related to the optical polarization fraction in V, p_V, through $R_{P/p} = P_S/p_V = 5.6 \pm 0.4$ MJy sr^{-1} (Planck Collaboration et al. 2014b). In the direction of EXO 2030+375, $\log P_S$ is estimated to be $\log P_S \sim -(1-0.3)$ MJy sr^{-1} (see Fig. 2 in Planck Collaboration et al. 2014a). Thus, the polarization fraction due to the ISM, according to *Planck* results, is again $p_V \lesssim 9\%$.
- *Field stars*. We measured the q and u Stokes parameters of 12 stars in the Robopol field of view not blocked by the mask in the target images. To reduce the uncertainty in the Stokes parameters of these stars, we combined several images when EXO 2030+375 was at the center of the instrument mask. The values were median filtered (averaged in case of 2) measurements of the same star. The main criterion for the selection of these stars was to have the four light spots free of nearby sources to avoid overlapping, signal-to-noise ratio in flux larger than 10, and the change in the polarization angle is lower than 30°. Figure 2 shows the $q-u$ plane of the field stars and the target. The four field stars for which dedicated observations were obtained (see Table 1) are also displayed with blue filled squares. Of all the sources, EXO 2030+375 (filled red circles) occupies the most distant position from the origin, indicating that it is the star with the highest polarization degree. Some field stars also display non-zero values of the Stokes parameters, but all the stars have $P_R \lesssim 9\%$, that is, the measured polarization degree of the stars in the vicinity of EXO 2030+375 agrees very well with what it is expected from the polarization-extinction relationship.
- *Wavelength dependence of the ISM polarization*. The spectrum of the ISM polarization obeys a well known empirical law given by $P(\lambda)/P_{\rm max} = \exp[-k\ln^2(\lambda_{\rm max}/\lambda)]$ (Serkowski, Mathewson & Ford 1975). It peaks in the optical band and falls both in the UV and near IR regions. $\lambda_{\rm max}$ is the wavelength at which $P_{\rm max}$ is observed and k is a measure of the sharpness of the spectrum. $\lambda_{\rm max}$ has been seen to correlate with the total to selective galactic extinction R_V as (see e.g. Whittet & van Breda 1978)

$$R_V = A_V/E(B-V) = (5.6 \pm 0.3)\,\lambda_{\rm max} \quad (1)$$

where $\lambda_{\rm max}$ is given in μm . The presence of an intrinsic polarization component can be inferred if the wavelength dependence of the ISM polarization is different from that of the established curve related to interstellar effects. Because the polarization from the interstellar medium is supposed to be constant with time, we can use the results in the J and K bands from Norton et al. (1994) together with our observation in the R band to estimate the total to selective extinction from eq. (1). The aim is to check whether the polarimetric data gives a value of R_V consistent with the average galactic value of $R_V = 3.1$ (Cardelli, Clayton & Mathis 1989). Assuming that $P(R) = 19.0\pm0.5\%$, $P(J) = 10.0\pm0.6\%$, and $P(K) = 4.2\pm0.2\%$ are entirely caused by the ISM, then

$$\frac{p_R}{p_J} = \frac{exp[-k\ ln^2(\lambda_{\rm max}/\lambda_R)]}{exp[-k\ ln^2(\lambda_{\rm max}/\lambda_J)]} \quad (2)$$

and equivalently for the K band

$$\frac{p_R}{p_K} = \frac{exp[-k\ ln^2(\lambda_{\rm max}/\lambda_R)]}{exp[-k\ ln^2(\lambda_{\rm max}/\lambda_K)]} \quad (3)$$

Dividing equation 2 by 3 and solving for $\lambda_{\rm max}$ we obtain $R_V = 0.77^{+0.75}_{-0.41}$, with a 3σ upper limit of $R_V = 2.62$, which is not consistent with the standard ratio of total to selective extinction of $R_V = 3.1$ (Cardelli, Clayton & Mathis 1989). Thus, either the extinction toward EXO 2030+375 is peculiar and does not obey the

average galactic extinction law or the observed polarization cannot be explained by the ISM.

Taking all the above considerations into account, we conclude that the ISM in the direction of EXO 2030+375 cannot explain the observed polarization degree.

3.2 Polarization in EXO 2030+375

Models that attempt to explain the polarization observed in Be stars as Thomson scattering predict maximum polarization fraction of 3–4%. Observations of classical Be stars agree with this value (see e.g. Yudin 2001). From the previous discussion we conclude that it is extremely unlikely that the interstellar medium can account for the measured polarization in EXO 2030+375. With the available data, it is difficult to separate the interstellar contribution from the observed polarization. As a rough approximation, we can assume that the measured polarization of the field stars is entirely of interstellar origin. We then calculate the average polarization degree of the nearby stars and subtract it vectorially from the total observed polarization (see e.g. Clarke 2010). The result is that ∼16% must be intrinsic. Such a high degree of polarization implies that a mechanism other than Thomson scattering might be at work in EXO 2030+375.

The main difference between an isolated Be star and a BeXB is the presence of a neutron star with a strong magnetic field. One is tempted to attribute the high polarization degree to this magnetic field. The alingment of non-spherical iron grains by the neutron star magnetic field might be an alternative mechanism to explain the high polarization in EXO 2030+375. The presence of iron in the Be discs is well documented. High resolution optical spectra of Be stars reveal the presence of Fe II emission lines with the strongest transitions in the optical band at λ5169 Å, λ4584 Å, and λ5317 Å (Hanuschik et al. 1996). In addition, BeXB in general and EXO 2030+375 in particular, show strong ($EW \sim 0.18$ keV) emission line in the X-ray spectra at 6.4-6.6 keV (Reynolds, Parmar & White 1993; Reig & Coe 1999). This line is interpreted as reprocessing of the hard X-ray continuum in relatively cool matter. Near-neutral iron generates a line centered at 6.4 keV, while this energy increases as the ionization stage increases. Therefore the detection of an iron line implies the presence of relatively cold matter in the vicinity of the X-ray source, which in the case of BeXB is the circumstellar disc.

For the proposed mechanism to work, two conditions have to be met: *i)* temperatures below the iron condensation[1] critical value are needed and *ii)* the neutron star has to physically interact with the disc.

The condensation temperature of iron is $\sim$ 1300 K (Savage, Cardelli & Sofia 1992). Above this temperature no grains can be formed because refractory elements like Fe cannot condense out of the gas phase. Models of the temperature structure of viscous discs in Be stars show that those discs are highly non-isothermal, mainly in the inner denser parts (Carciofi & Bjorkman 2006). When the density is large enough ($\rho_0 \gtrsim 5 \times 10^{-12}$ g cm^{-3}) the disc develops a cool equatorial region close to the star. As the density increases, the minimum temperature decreases and moves further away from the central star (Carciofi & Bjorkman 2008; Sigut, McGill & Jones 2009). Still the lowest temperature predicted by the model for a B0 star is 6000–8000 K, well above the temperature for grain condensation of iron. However, these simulations predict the temperature profile relatively close to the star, whereas the temperature in the outermost regions, where the disc meets the interstellar space, is expected to be significantly lower and so is the particle density content.

A dipolar magnetic field decreases with distance as $B = B_0(R_{\rm NS}/r)^3$, where B_0 is the neutron star polar magnetic field. This pronounced decrease of the strength of the magnetic field with distance implies that the disc feels a substantial magnetic field only when the radius of the disc is comparable to the periastron distance. The Hα equivalent width of EXO 2030+375 varies in the range 8-20 Å (Norton et al. 1994; Reig et al. 1998; Baykal et al. 2008), which implies a disc radius of the order of $R_{\rm disc} \gtrsim 10R_*$ (Grundstrom & Gies 2006; Carciofi 2011). Also, Monte Carlo simulations that attempt to reproduce the continuum polarization in equatorial discs show that polarization is formed far away from the star. Approximately 95% of the maximum polarization is reached only when the disc size is about ten stellar radii (Carciofi 2011). Assuming a stellar radius of $R_* \approx 8$ R$_\odot$ for a B0V star, the disc radius would be $R_{\rm disc} \sim 5.5 \times 10^{12}$ cm, which roughly coincides with the periastron distance using the orbital solution of Wilson, Finger & Camero-Arranz (2008) and assuming a stellar mass $M_* = 16$ M$_\odot$.

Further evidence for close encounters between the neutron star and the disc during periastron comes from the X-rays. EXO 2030+375 is unique among other BeXBs in that it shows stable and long-lasting periodic X-ray type I outbursts (Wilson, Finger & Camero-Arranz 2008). This suggests that the neutron star physically interacts with the disc at every periastron passage. With a typical magnetic field of $\sim 10^{12}$ G (Reig & Coe 1999; Wilson, Finger & Camero-Arranz 2008), the alignment efficiency is very high and the iron grains get magnetized very fast. Because the iron grains are inmersed in a gas, gas-grain collisions tend to restore random orientation. Thus, whether the alignment survives throughout the orbital period depends on the relaxation time, which in turn depends on the size of the grains and the temperature and particle density of the gas (see eq. (4.26) in Whittet 1992). For the typical parameters expected in a Be star disc, the relaxation time-scales are of the order of tens of days to years. In this scenario, we would expect to observe orbital polarimetric variability when the relaxation time is smaller than the orbital period. The lack of orbital variability in EXO 2030+375 indicates that the continuous passages of the neutron star through periastron ensures that the grain alignment in the outer parts of the disc is not lost.

A prediction of the model is that polarization and X-ray activity must correlate in BeXBs, in the sense that a high degree of polarization should be observed during type I outbursts.

4 CONCLUSION

We have performed optical (R band) polarimetric and photometric observations of the Be/X-ray binary EXO 2030+375 and found the highest optical polarization degree ever reported in a Be star. Over a year the source has shown a fairly constant level of polarization at $\sim$ 19% and polarization angle of 40°. We have shown evidence indicating that the contribution of the interstellar medium cannot account for the total measured polarization, leaving room for a large intrinsic contribution. This evidence is based on the inconsistent value of the total to selective extinction R_V obtained assuming that *all* the measured polarization is due to the ISM, the relationship

[1] The condensation temperature of an element is defined as the temperature at which half of that element is removed from the gas phase due to the formation of solid condensates (Savage, Cardelli & Sofia 1992).

between polarization and extinction in the ISM, and the measured polarization of stars in the vicinity of the target. The origin of the polarized light in EXO 2030+375 is not clear, but a different mechanism from that proposed in classical Be stars must be invoked.

ACKNOWLEDGMENTS

RoboPol is a collaboration involving the University of Crete, the Foundation for Research and Technology - Hellas, the California Institute of Technology, the Max-Planck Institute for Radioastronomy, the Nicolaus Copernicus University, and the Inter-University Centre for Astronomy and Astrophysics. This work was partially supported by the "RoboPol" project, which is implemented under the "Aristeia" Action of the "Operational Programme Education and Lifelong Learning" and is co-funded by the European Social Fund (ESF). We also acknowledge support from the COST Action MP1104 "Polarisation as a tool to study the Solar System and beyond". K.T. acknowledges support by FP7 Marie Curie Career Integration Grant PCIG-GA-2011-293531 "SFOnset" and the EU FP7 Grant PIRSES-GA-2012-31578 "EuroCal".

REFERENCES

Baykal A., Kızıloğlu Ü., Kızıloğlu N., Beklen E., Özbey M., 2008, A&A, 479, 301
Carciofi A. C., 2011, in IAU Symposium, Vol. 272, IAU Symposium, Neiner C., Wade G., Meynet G., Peters G., eds., pp. 325–336
Carciofi A. C., Bjorkman J. E., 2006, ApJ, 639, 1081
Carciofi A. C., Bjorkman J. E., 2008, ApJ, 684, 1374
Cardelli J. A., Clayton G. C., Mathis J. S., 1989, ApJ, 345, 245
Clarke D., 2010, Stellar Polarimetry
Coe M. J., Payne B. J., Longmore A., Hanson C. G., 1988, MNRAS, 232, 865
Dachs J., Kiehling R., Engels D., 1988, A&A, 194, 167
Fitzgerald M. P., 1970, A&A, 4, 234
Fosalba P., Lazarian A., Prunet S., Tauber J. A., 2002, ApJ, 564, 762
Gehrz R. D., Hackwell J. A., Jones T. W., 1974, ApJ, 191, 675
Grundstrom E. D., Gies D. R., 2006, ApJ, 651, L53
Gutierrez-Moreno A., 1979, PASP, 91, 299
Halonen R. J., Mackay F. E., Jones C. E., 2013, ApJS, 204, 11
Hanuschik R. W., Hummel W., Sutorius E., Dietle O., Thimm G., 1996, A&AS, 116, 309
Hiltner W. A., 1956, ApJS, 2, 389
Janot-Pacheco E., Motch C., Pakull M. W., 1988, A&A, 202, 81
Jones T. J., 1989, ApJ, 346, 728
Jones T. J., Gehrz R. D., 1990, AJ, 100, 274
King O. G. et al., 2014, MNRAS, 442, 1706
Krautter J., 1980, A&A, 89, 74
Landolt A. U., 1992, AJ, 104, 340
Landolt A. U., 2009, AJ, 137, 4186
Motch C., Janot-Pacheco E., 1987, A&A, 182, L55
Norton A. J. et al., 1994, MNRAS, 271, 981
Okazaki A. T., Bate M. R., Ogilvie G. I., Pringle J. E., 2002, MNRAS, 337, 967
Parmar A. N., White N. E., Stella L., Izzo C., Ferri P., 1989, ApJ, 338, 359
Planck Collaboration et al., 2014a, ArXiv e-prints
Planck Collaboration et al., 2014b, ArXiv e-prints
Porter J. M., Rivinius T., 2003, PASP, 115, 1153
Reig P., 2011, Ap&SS, 332, 1
Reig P., Coe M. J., 1999, MNRAS, 302, 700
Reig P., Stevens J. B., Coe M. J., Fabregat J., 1998, MNRAS, 301, 42
Reynolds A. P., Parmar A. N., Stollberg M. T., Verbunt F., Roche P., Wilson R. B., Finger M. H., 1996, A&A, 312, 872
Reynolds A. P., Parmar A. N., White N. E., 1993, ApJ, 414, 302
Rivinius T., Carciofi A. C., Martayan C., 2013, A&A Rev., 21, 69
Savage B. D., Cardelli J. A., Sofia U. J., 1992, ApJ, 401, 706
Serkowski K., Mathewson D. S., Ford V. L., 1975, ApJ, 196, 261
Sigut T. A. A., McGill M. A., Jones C. E., 2009, ApJ, 699, 1973
Waters L. B. F. M., Marlborough J. M., 1992, A&A, 256, 195
Wegner W., 1994, MNRAS, 270, 229
Wegner W., 2006, MNRAS, 371, 185
Whittet D. C. B., 1992, Dust in the galactic environment
Whittet D. C. B., van Breda I. G., 1978, A&A, 66, 57
Wilson C. A., Finger M. H., Camero-Arranz A., 2008, ApJ, 678, 1263
Wilson C. A., Finger M. H., Coe M. J., Laycock S., Fabregat J., 2002, ApJ, 570, 287
Wood K., Bjorkman J. E., Whitney B. A., Code A. D., 1996, ApJ, 461, 828
Yudin R. V., 2001, A&A, 368, 912